Sustainable depletion of high-abundance serum proteins using aqueous biphasic systems based on glycine-betaine analogue ionic liquids for the detection of masked biomarkers

Matheus M. Pereira , Sónia N. Pedro , Francisca A. e Silva , Aminou Mohamadou , João A.P. Coutinho , Mara G. Freire

PII: S0021-9673(26)00385-7
DOI: https://doi.org/10.1016/j.chroma.2026.467055
Reference: CHROMA 467055

To appear in: *Journal of Chromatography A*

Received date: 10 February 2026
Revised date: 29 April 2026
Accepted date: 29 April 2026

Please cite this article as: Matheus M. Pereira , Sónia N. Pedro , Francisca A. e Silva , Aminou Mohamadou , João A.P. Coutinho , Mara G. Freire , Sustainable depletion of high-abundance serum proteins using aqueous biphasic systems based on glycine-betaine analogue ionic liquids for the detection of masked biomarkers, *Journal of Chromatography A* (2026), doi: https://doi.org/10.1016/j.chroma.2026.467055

Sustainable depletion of high-abundance serum proteins using aqueous biphasic systems based on glycine-betaine analogue ionic liquids for the detection of masked biomarkers

Matheus M. Pereira[a], Sónia N. Pedro[a], Francisca A. e Silva[a]*, Aminou Mohamadou[b], João A. P. Coutinho[a] and Mara G. Freire[a]*

[a]*CICECO – Aveiro Institute of Materials, Department of Chemistry, University of Aveiro, 3810-193 Aveiro, Portugal*

[b]*Universite de Reims Champagne-Ardenne, Institut de Chimie Moleculaire de Reims (ICMR), CNRS UMR 7312, UFR des Sciences Exactes et Naturelles, BP 1039, F-51687 Reims cedex 2, France*

*Corresponding author: E-mail: maragfreire@ua.pt, francisca.silva@ua.pt

Abstract

The detection of protein biomarkers in human serum using more sustainable analytical strategies remains constrained by the predominance of high-abundance proteins, particularly human serum albumin (HSA) and immunoglobulin G (IgG), which limits access to low-abundance targets. To address these limitations, aqueous biphasic systems (ABS) comprising glycine-betaine analogue ionic liquids (AGB-ILs) are introduced as a green sample preparation strategy for the selective depletion of high-abundance serum proteins. After synthesizing and characterizing AGB-ILs, including their thermal properties and ecotoxicity, these were combined with a citrate buffer and screened for ABS formation. HSA and IgG were efficiently depleted in a single step via interfacial precipitation, allowing the detection of previously suppressed analytes such as transferrin using size-exclusion high-performance liquid chromatography with UV detection (SE-HPLC-UV). This demonstrates that effective sample pretreatment can enable the use of simpler analytical techniques compared to immunoassay- and mass spectrometry-based approaches. The sustainability profile of the proposed approach was evaluated using the AGREE (Analytical GREEnness), AGREEprep (Analytical GREEnness for sample PREParation), and BAGI (BioAnalytical Greenness Index) metrics, confirming low toxicity, reduced reagent consumption, and potential for improved workflow integration. Ultimately, this work extends the applicability of IL-based ABS for protein depletion, establishing bio-inspired ILs as promising tools for green bioanalytical workflows.

Keywords: Ionic liquid; Aqueous biphasic system; Sample pretreatment; Protein depletion; Biomarker

1. Introduction

The advancement of biomedicine plays a crucial role in monitoring, diagnosing, and managing diseases, with technological progress in proteomics and genomics improving modern healthcare [1]. The detection of gene and protein biomarkers in human fluids provides valuable insights into health conditions [1]. However, compared with genomics, proteomics faces challenges due to the complexity and dynamic nature of human fluids, particularly in detecting protein biomarkers [2,3]. Plasma and serum, the preferred fluids for bioanalysis, contain a highly intricate proteomic profile dominated by high-abundance proteins like human serum albumin (HSA) and immunoglobulin G (IgG), which together constitute over 75% of the total protein content [4–6]. These species interfere with the detection of target proteins present at lower concentrations, affecting analytical techniques such as immunoassays and mass spectrometry. Additionally, the inherent lability of protein biomarkers increases the risk of denaturation and degradation, further compromising detection accuracy and reproducibility [7,8]. Overcoming these limitations often demands highly specialized techniques that are time-intensive, costly, and require expert handling [7,8]. Consequently, effective sample pretreatment, encompassing depletion, fractionation, and enrichment strategies, is essential to ensure reliable bioanalysis [9].

This work focuses on the depletion stage of sample pretreatment, which involves removing high-abundance proteins to enhance the detection and identification of target analytes. Solid-phase extraction using dyes, proteins, and immunoaffinity ligands has been widely employed and is commercially available in user-friendly kit formats [9]. However, these methods are often limited by non-specific binding and an inability to distinguish isoforms, resulting in modest efficiency, yield, and selectivity [9]. Furthermore, their high cost and limited sample loading capacity hinder broader application and compromise their sustainability [9]. Protein precipitation using polymers, salts, and organic solvents is a simpler depletion strategy, but it often results in the loss of target analytes [10].

The drawbacks associated with these standard approaches can be addressed by employing aqueous biphasic systems (ABS), or aqueous two-phase systems (ATPS) [11]. ABS are liquid-liquid extraction techniques that typically eliminate the need for volatile

organic solvents in their formation. Instead, they rely on mixing two components (usually two polymers or a polymer and a salt) in water above specific concentrations [12]. ABS stand out from other liquid-liquid extraction methods because of their water-rich environment and highly tunable formulations [12]. As a result, they provide adequate conditions for extracting biomarkers from biological fluids, such as proteins [13–16] and extracellular vesicles [17–19]. However, polymeric ABS are limited by phase viscosity, polarity range, and poor selectivity, which hinder the complete isolation of target analytes in a single step [17,19]. Accordingly, additional purification steps and the use of specialized equipment may be required, presenting significant obstacles to the widespread adoption of polymeric systems in clinical laboratory analysis [18].

Ionic liquids (ILs), with their customizable solvent properties, have emerged as valuable components in ABS, offering enhanced performance in biological sample processing, particularly in single-step configurations [20]. The extensive variety of cation-anion combinations and phase-forming component pairs in IL-based ABS provides a flexible platform for optimizing protein depletion and improving analyte recovery in sample pretreatment applications [21]. With the growing interest in bio-inspired ILs, such as those derived from choline and amino acids, these systems have become more closely aligned with Green Analytical Chemistry principles, contributing to a reduced environmental impact in bioanalytical processes [22–25]. Additionally, ABS formed with bio-inspired ILs tend to provide gentler conditions, preserving the integrity of sensitive biomolecules, such as proteins, while ensuring efficient and selective extraction of target analytes and minimizing degradation risks [26].

Among bio-inspired alternatives, ILs with glycine-betaine-type cationic cores – hereafter referred to as glycine-betaine analogue ILs (AGB-ILs) – also serve as viable phase-forming components of ABS [27,28]. From a Green Sample Preparation perspective [24], AGB-ILs benefit from their structural resemblance to naturally occurring amino acid derivatives (aligning with principle 2 – *Use safer solvents and reagents* – and principle 10 of Green Sample Preparation – *Ensure safe procedures for the operator*) [27–30]. Furthermore, AGB-ILs confer higher cost-effectiveness and performance in ABS formation, particularly when compared to their imidazolium-based congeners, as they require lower amounts of phase-forming components (adhering to principle 5 of Green Sample Preparation – *Minimize sample, chemical and material*

amounts) [27]. The relatively higher hydrophobicity of AGB-ILs while remaining water-miscible may favor interfacial depletion of interfering biological molecules, facilitating potential integration of depletion, fractionation, and enrichment stages of sample pretreatment in a single step (in line with principle 7 of Green Sample Preparation – *Integrate steps and promote automation*) [21,27,30].

Supported by the properties of IL-based ABS, further enhanced by bio-inspired ILs, this work reports the depletion of high-abundance proteins from human serum, leading to the detection of previously undetected proteins. Instead of relying on imidazolium-, ammonium-, or phosphonium-based ILs used previously [21], AGB-ILs are considered here to better align with Green Sample Preparation principles [24]. Although the use of AGB-ILs as phase-forming components is an incremental advance in IL-based sample pretreatment [21], the main contribution of this work lies in the analytical strategy driven by ABS-mediated depletion. This strategy is based on the use of size exclusion high-performance liquid chromatography coupled with UV detection (SE-HPLC-UV) for bioanalysis, where target proteins would otherwise remain masked by high-abundance serum components. In this context, the proposed pretreatment strategy enables the use of simpler analytical techniques, minimizing reliance on conventional immunoassays or mass spectrometry for serum protein detection. By the informed design of AGB-ILs, which is accomplished here through their synthesis, physicochemical characterization, toxicity assessment, and ABS ternary phase diagrams determination in the presence of a salt buffer, the depletion of high-abundance proteins HSA and IgG is projected at the ABS interphase through precipitation. Following depletion, the detection of transferrin in the AGB-IL-rich phase is revealed, confirming the potential of the proposed analytical workflow. To assess the sustainability and operational performance of the proposed method, complementary metrics – AGREE (Analytical GREEnness [31]), AGREEprep (Analytical GREEnness for sample PREParation [32]), and BAGI (BioAnalytical Greenness Index [33]) – were applied to evaluate reagent safety, waste generation, energy use, and analytical accessibility, in line with Green and White Analytical Chemistry [34,35].

2. Materials and Methods

2.1. Materials

For the synthesis of AGB-ILs, all tertiary amines (*N*-methylpyrrolidine, purity ≥ 97 wt%, CAS 120-94-5; triethylamine, purity ≥ 99 wt%, CAS 121-44-8; tripropylamine, purity ≥ 98 wt%, CAS 102-69-2; tributylamine, purity ≥ 98 wt%, CAS 102-82-9), ethyl acetate (purity ≥ 99.5 wt%, CAS 141-78-6), ethyl ether (purity ≥ 99.0 wt%, CAS 60-29-7), 4-bromobutyrate acid ethyl ester (purity ≥ 97 wt%, CAS 2969-81-5) and bromoacetic acid ethyl ester (purity = 98 wt%, CAS 105-36-2) were acquired from Sigma-Aldrich. Silver saccharinate (CAS 2673-17-8), silver lactate (CAS 15768-18-0), silver pyruvate (CAS 62163-16-0), silver dicyanamide (CAS 51342-29-1) and silver salicylate (CAS 528-93-8) were prepared from mixtures (mole ratio of 1:1.1) of silver nitrate ($AgNO_3$, purity ≥ 99.0 wt%, CAS 7761-88-8) and the respective sodium salt, all from Sigma-Aldrich: sodium saccharinate (purity ≥ 97 wt%, CAS 128-44-9), sodium lactate (purity ≥ 99.0 wt%, CAS 72-17-3), sodium pyruvate (purity ≥ 99 wt%, CAS 113-24-6), sodium dicyanamide (purity ≥ 97.0 wt%, CAS 1934-75-4) and sodium salicylate (purity ≥ 99.5 wt%, CAS 54-21-7). The buffer used in ABS preparation was made of potassium citrate ($K_3C_6H_5O_7{\cdot}H_2O$, purity ≥ 99 wt%, CAS 6100-05-6) from Sigma-Aldrich, and citric acid ($C_6H_8O_7{\cdot}H_2O$, purity = 100 wt%, CAS 5949-29-1) from Fisher Scientific.

Pure IgG (purity ≥ 95 wt%, CAS 9007-84-5) and human transferrin (purity ≥ 98 wt%, CAS 11096-37-0) were both acquired from Sigma-Aldrich, while HSA (purity = 96 wt%, CAS 70024-90-7) was purchased from Alfa Aesar. Human serum was acquired at Sigma-Aldrich as a pooled sample from multiple donors, providing an average composition representative of a typical human serum matrix. This sample allows a reliable proof-of-concept evaluation of the ABS-mediated depletion workflow for bioanalytical applications.

The mobile phase used in HPLC analysis was composed of sodium phosphate dibasic heptahydrate ($Na_2HPO_4{\cdot}7H_2O$, purity = 98−102 wt%, CAS 7782-85-6), sodium phosphate monobasic (NaH_2PO_4, purity = 99−100.5 wt%, CAS 7558-80-7), and sodium chloride (NaCl, purity = 99.5 wt%, CAS 7647-14-5), all acquired from Panreac AppliChem. SDS-PAGE molecular weight standards, namely marker molecular weight full-range were

acquired at VWR. Ultra-pure water (CAS 7732-18-5) which was double distilled and then treated with a Milli-Q plus 185 water purification apparatus was used for the SE-HPLC analysis. The Human Transferrin Enzyme Linked Immunosorbent Assay (ELISA) kit (ab187391) was from Abcam.

2.2. Synthesis and characterization of AGB-ILs

The synthetic pathway for AGB-ILs (cf. Figure S1, Supplementary Material) starts via the reaction of corresponding tertiary amine and ethyl bromo-*n*-alkanoate to obtain Br-based AGB-ILs, as previously reported [27,36]. Subsequently, metathesis of Br-based AGB-ILs was performed to obtain the newly synthesized AGB-ILs investigated in this work. Detailed information on the synthesis of each specific AGB-IL can be found in the Supplementary Material. Figure 1 shows the chemical structures of all AGB-ILs used in this work.

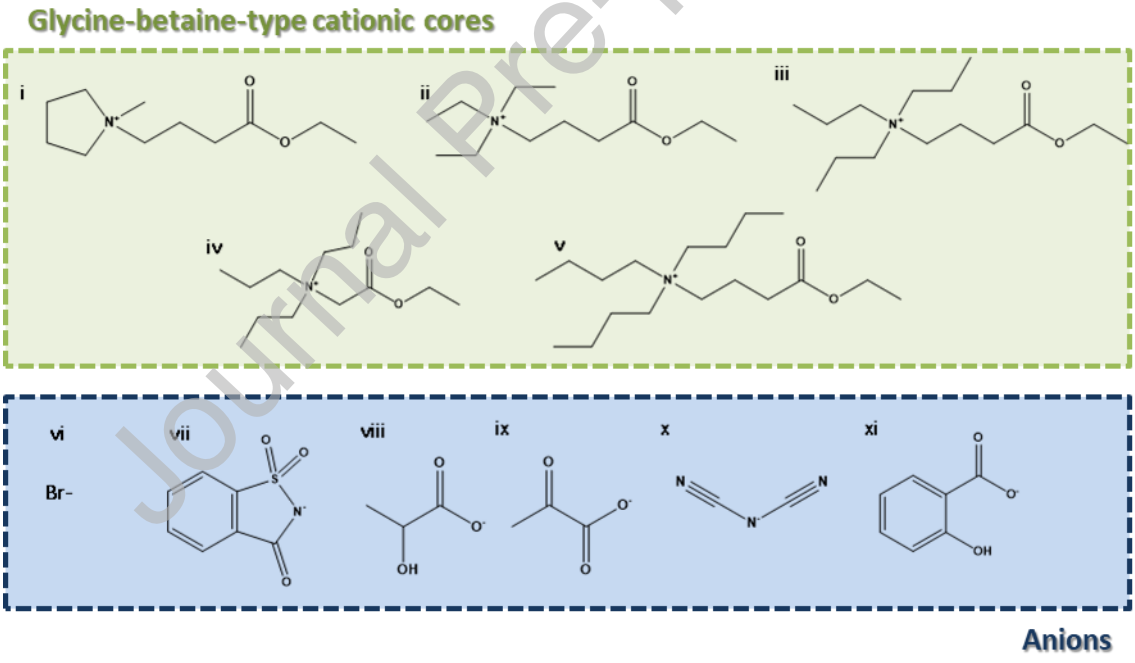

Figure 1. Chemical structures of AGB-ILs constituting ions: (i) $[MepyrNC_4]^+$, (ii) $[Et_3NC_4]^+$, (iii) $[Pr_3NC_4]^+$,(iv) $[Pr_3NC_2]^+$, (v) $[Bu_3NC_4]^+$, (vi) Br^-, (vii) $[Sac]^-$, (viii) $[Lac]^-$, (ix) $[Pyr]^-$, (x) $[Dca]^-$ and (xi) $[Sal]^-$.

Characterization of AGB-ILs was performed after vacuum-drying them to a final water content below 0.06 wt%, quantified by Karl Fischer coulometry (Metrohm 787 KF Titrino) with Hydranal 34805 and Hydranal 37817 (Fluka) as titrant. Elemental analyses

(C, H, N and S contents) of all synthesized ILs were carried on a PerkinElmer 2400 C, H, N and S element analyzer. ^{1}H and ^{13}C Nuclear magnetic resonance (NMR) were recorded at room temperature with a Bruker AC 30 spectrometer (250 MHz for ^{1}H, 62.5 MHz for ^{13}C) using DMSO-d_6 as solvent. The melting points and decomposition temperatures of the AGB-ILs were determined by thermal analysis using a thermogravimetric analyzer with differential scanning calorimetry capability (Mettler Toledo TGA/DSC 1 LF). The instrument was calibrated with indium (purity ≥ 99.99 wt%, CAS 7440-74-6) as the standard, and all measurements were analyzed using STAR software. The samples were prepared in the aluminum pans and heated from 303.15 to 873.15 K, with a heating rate of 5 K·min^{-1} and under nitrogen gas flow of 40 mL·min^{-1}. The standard uncertainty of temperature is 0.2 K.

The toxicity of AGB-ILs was assessed using the Standard Microtox® liquid-phase bioassay [37]. Microtox® is based on the bioluminescence inhibition of *Aliivibrio fischeri* (*A. fischeri*) (strain NRRL B- 11177) after exposure to AGB-ILs solutions at 15 °C. The standard 81.9 % test protocol was followed, where *A. fischeri* is exposed to a range of diluted aqueous solutions of each AGB-IL (i.e., from 0 to 81.9 wt%, taking 100% as the concentration of AGB-IL stock solutions prepared). After 5, 15, and 30 min of exposure to each aqueous solution, the bioluminescence emission of *A. fischeri* was measured and related to that of a blank control. The data were fitted using non-linear regression by the least-squares method, allowing EC_{50} values to be determined at 5, 15, and 30 minutes of exposure. EC_{50} (Median Effective Concentration) refers to the estimated concentration required to induce a 50 % inhibition of bioluminescence, calculated with a 95 % confidence interval.

2.3. Determination of AGB-IL-based ABS ternary phase diagrams

Aqueous solutions of each AGB-IL at *circa* 90 wt% and aqueous solutions of the $K_3C_6H_5O_7/C_6H_8O_7$ mixture (as a buffer solution at pH ≈ 7, mole ratio of ≈ 15:1, discounting the complexed water in both $K_3C_6H_5O_7{\cdot}H_2O$ and $C_6H_8O_7{\cdot}H_2O$) at ≈ 50 wt% were used for the determination of binodal curves by the well-established cloud point titration method at 25 °C and under atmospheric pressure [27]. Alternate drop-wise addition of $K_3C_6H_5O_7/C_6H_8O_7$ aqueous solution and of pure water to the AGB-IL aqueous solution was repeatedly carried under constant stirring. This procedure allows the consecutive

attainment of the biphasic region (turbid solution) and the monophasic region (translucent solution), respectively. Each drop addition step is followed by weight quantification (±10^{-4} g) of all components in solution, so that ternary systems compositions are determined.

Experimental data of ABS binodal curves were fitted using Equation 1, initially proposed by Merchuk et al. [38]:

$$[AGB\text{-}IL] = Aexp[(B[salt]^{0.5}) - (C[salt]^3)] \quad (1)$$

where $[AGB\text{-}IL]$ and $[salt]$ are AGB-IL and salt weight fraction percentages, respectively, and A, B, and C are fitting constants.

To fully characterize ABS phase diagrams, tie-lines (TLs) were determined by a gravimetric method originally proposed by Merchuk et al. [38], which has been widely employed and validated in the context of IL-salt-based ABS [39]. Two biphasic mixture points per ternary phase diagram were prepared, vigorously stirred, centrifuged for 10 min and allowed to reach equilibrium by the separation of the phases for at least 10 min at 25 °C. After separation, both top and bottom phases were weighed. For all systems, the top phase corresponds to an AGB-IL-rich phase, whereas the bottom phase is mainly constituted by $K_3C_6H_5O_7$/$C_6H_8O_7$. Each individual TL was determined by the lever-arm rule, where the relationship between the top AGB-IL-rich phase and the overall system weight is applied. The determination of TLs was accomplished by solving the following system of four equations (Equations 2 to 5) and four unknown variables ($[AGB\text{-}IL]_{AGB\text{-}IL}$, $[AGB\text{-}IL]_{salt}$, $[salt]_{AGB\text{-}IL}$ and $[salt]_{salt}$):

$$[AGB\text{-}IL]_{salt} = Aexp[(B[salt]^{0.5}_{AGB\text{-}IL}) - (C[salt]^3_{AGB\text{-}IL})] \quad (2)$$

$$[AGB\text{-}IL]_{salt} = Aexp\left[\left(B[salt]^{0.5}_{salt}\right) - (C[salt]^3_{salt})\right] \quad (3)$$

$$[AGB\text{-}IL]_{AGB\text{-}IL} = \frac{[AGB\text{-}IL]_M}{\alpha} - \frac{1-\alpha}{\alpha}[AGB\text{-}IL]_{salt} \quad (4)$$

$$[salt]_{AGB\text{-}IL} = \frac{[salt]_M}{\alpha} - \frac{1-\alpha}{\alpha}[salt]_{salt} \quad (5)$$

where the subscripts "*AGB-IL*", "*salt*" and "*M*" denote the top AGB-IL-rich phase, the bottom salt-rich phase, and the overall mixture, respectively. α denotes the ratio between the weight of the top AGB-IL-rich phase and that of the overall mixture. The tie-line length (TLL) is the Euclidian distance between the top AGB-IL-rich and bottom salt-rich phase compositions and is calculated using Equation 6.

$$TLL = \sqrt{([salt]_{AGB\text{-}IL} - [salt]_{salt})^2 + ([AGB\text{-}IL]_{AGB\text{-}IL} - [AGB\text{-}IL]_{salt})^2} \quad (6)$$

In binodal curves representations and TLs determinations, the salt composition refers only to $C_6H_5K_3O_7$ and $C_6H_8O_7$ content, while the water content of the buffer is considered as part of the ternary system water composition.

2.4. Serum protein depletion and transferrin extraction using AGB-IL-based ABS

Biphasic mixtures were prepared at a fixed composition consisting of 30 wt% of AGB-IL + 60 wt% of citrate buffer solution ($K_3C_6H_5O_7$/$C_6H_8O_7$ at 50 wt%, pH 7) + 10 wt% of human serum (as received), with variation restricted to the structure of the AGB-IL. Each mixture was prepared to a final mass of 2 g as previously described and allowed to equilibrate under the established conditions. While HSA and IgG were depleted via precipitation at the ABS interphase, the top and bottom phases were carefully separated for their quantification by SE-HPLC-UV. A Chromaster chromatograph (VWR Hitachi) equipped with a size-exclusion column (Shodex Protein KW-802.5; 8 mm × 300 mm) was used. The mobile phase was composed of a phosphate buffer (pH 7, 100 mM) and NaCl (0.3 M) aqueous solutions. Analytical separation was conducted using isocratic elution at a flow rate of 1 mL·min^{-1} and the injection volume was 25 µL. The column oven and auto-sampler were kept at 25 °C. The UV detector was set to measure at 280 nm. With a total analysis time of 40 min, the retention times of IgG and HSA were found to be at circa 15.7 and 17.1 min, respectively. Each aqueous phase was diluted at a 1:10 volume-to-volume (v/v) ratio in the mobile phase prior to injection. Blank controls of the ABS phases prepared without serum were routinely analyzed to account for potential interference from the IL and salt in the UV signal, ensuring accurate protein quantification. Quantifications were carried out by an external standard calibration method, with correlation coefficients (R^2) higher than 0.99 for both proteins supporting linearity. A summary of the analytical performance parameters, including the calibration concentration ranges and the limits of detection (LOD) and quantification (LOQ), is provided in Table S1 (Supplementary Material).

When no detectable signal of HSA or IgG was observed by SE-HPLC-UV, depletion was considered quantitative within the LODs of the method. Due to analytical challenges in directly analyzing the interphase in the studied systems, the amount of protein precipitated at the interphase was estimated using a mass balance approach, calculated

as the difference between the initial serum protein content and the protein remaining in the aqueous phases. This approach assumes ideal phase separation and negligible analyte losses during handling and may be affected by experimental limitations in the phase separation step, including potential cross-contamination between phases. Nevertheless, it provides a reliable determination of protein depletion and has been previously validated by us [21]. Experiments were carried out at least in duplicate, and, when quantitative depletion is observed in all replicates, no standard deviations are reported.

The depletion efficiency of HSA and IgG, $\boldsymbol{DE_{HSA}}\%$ and $\boldsymbol{DE_{IgG}}\%$ are the percentage ratio between the amount of protein in the solid interphase to that in the total mixture, and is defined according to Equations 7 and 8:

$$\boldsymbol{DE_{HSA}}\% = \frac{\boldsymbol{w_{HSA}^{Int}}}{\boldsymbol{w_{HSA}^{AGB\text{-}IL}+w_{HSA}^{Salt}+w_{HSA}^{Int}}} \times \mathbf{100} \quad (7)$$

$$\boldsymbol{DE_{IgG}}\% = \frac{\boldsymbol{w_{IgG}^{Int}}}{\boldsymbol{w_{IgG}^{AGB\text{-}IL}+w_{IgG}^{Salt}+w_{IgG}^{Int}}} \times \mathbf{100} \quad (8)$$

where $w_{HSA}^{AGB\text{-}IL}$, w_{HSA}^{Salt}, w_{HSA}^{Int}, $w_{IgG}^{AGB\text{-}IL}$, w_{IgG}^{Salt} and w_{IgG}^{Int} are the total weight of HSA or IgG in the AGB-IL-rich phase, salt-rich phase and solid interphase, respectively.

As a representative system, the phases of the ABS composed of 30 wt% of $[Bu_3NC_4]Br$ + 60 wt% of citrate buffer ($K_3C_6H_5O_7/C_6H_8O_7$ at 50 wt%, pH 7) + 10 wt% of human serum were analyzed in terms of human transferrin concentration. This analysis was done by SE-HPLC-UV, resorting to the previously mentioned conditions and a preestablished linear calibration curve (Table S1, Supplementary Material). Also, the concentration of transferrin in the original serum sample was determined by ELISA according to the manufacturer's instructions, and found to be 1.8 ± 0.1 $g \cdot L^{-1}$, in agreement with reference values [40].

The recovery yield of transferrin, $RY_{TF}\%$, to the AGB-IL-rich phase, was determined as follows:

$$\boldsymbol{RY_{TF}}\% = \frac{\boldsymbol{w_{TF}^{AGB\text{-}IL}}}{\boldsymbol{w_{TF}^{serum}}} \times \mathbf{100} \quad (9)$$

where $w_{TF}^{AGB\text{-}IL}$ is the total weight of transferrin in the AGB-IL-rich phase, and w_{TF}^{serum} is the total weight of transferrin in the original serum sample.

The relative error of quantification by SE-HPLC-UV after ABS-mediated depletion was determined using the following Equation:

$$Relative\ error\ \% = \frac{[TF]_{original\ serum} - [TF]_{depleted\ serum}}{[TF]_{original\ serum}} \quad (10)$$

where $[TF]_{original\ serum}$ is the concentration of transferrin in the original serum determined by ELISA, whereas $[TF]_{depleted\ serum}$ is the concentration of transferrin in the depleted serum sample determined by SE-HPLC.

The methodology described above supported the development of an analytical workflow for serum transferrin detection using SE-HPLC-UV. As schematically represented in Figure 2, processing serum with aqueous solutions of AGB-IL and citrate buffer efficiently depletes high-abundance proteins at a solid interphase, while the separated top (AGB-IL-rich) phase can be directly analyzed, enabling the quantification of previously masked biomarkers.

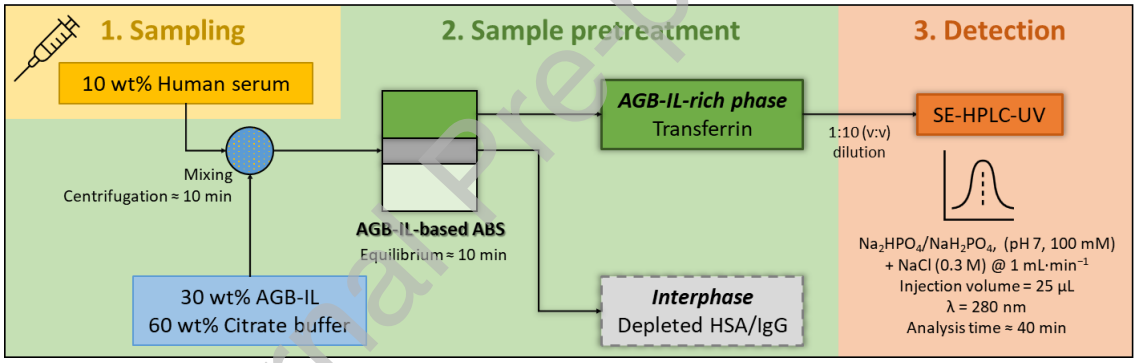

Figure 2. Analytical setup for the detection of previously masked protein biomarkers by SE-HPLC-UV after depletion using AGB-IL-based ABS.

2.5. Protein identification by sodium dodecyl sulphate polyacrylamide gel electrophoresis (SDS-PAGE)

Samples of each ABS phase were diluted at 2:1 (v/v) in a dissociation buffer consisting of 2.5 mL of 0.5 M Tris-HCl pH 6.8, 4.0 mL of 10 % (w/v) SDS solution, 2.0 mL of glycerol, 2.0 mg of bromophenol blue and 310 mg of dithiothreitol (DTT). This overall solution was heated at 95 °C for 5 min to denature proteins by reducing disulfide linkages and thus partially overcoming tertiary protein folding and disrupting quaternary protein structure. Electrophoresis was run on polyacrylamide gels (stacking: 4 % and

resolving: 20 %) with a running buffer constituted by 250 mM Tris-HCl, 1.92 M glycine, and 1 % SDS using an Amersham ECLTM Gel from GE Healthcare Life Sciences. The proteins were stained with Coomassie Brilliant Blue G-250 0.1 % (w/v), methanol 50 % (v/v), acetic acid 7 % (v/v) and water 42.9 % (v/v). All gels were placed in an orbital shaker at a moderate speed during 2-3 h at room temperature. The gels were further distained in a solution containing acetic acid at 7 % (v/v), methanol at 20 % (v/v) and water at 73 % (v/v) in an orbital shaker at a moderate speed during 3-4 h at room temperature. Molecular weight standards were used as protein standards. All gels were analyzed using the Image Lab 3.0 (BIO-RAD) analysis tool.

3. Results and discussion

3.1. Developing AGB-ILs for ABS formation

AGB-ILs studied are composed of glycine-betaine-type cationic cores, viz. 1-(4-ethoxy-4-oxobutyl)-1-methylpyrrolidin-1-ium ($[MepyrNC_4]^+$) and *N,N,N*-trialkyl(ω-ethoxy-ω-oxoalkyl)-1-ammonium ($[X_3NC_m]^+$, with X = ethyl, Et; propyl, Pr; and butyl, Bu; and *m* = 2, 4) combined with six different anions, namely bromide ($[Br]^-$), saccharinate ($[Sac]^-$), lactate ($[Lac]^-$), pyruvate ($[Pyr]^-$), dicyanamide ($[Dca]^-$) and salicylate ($[Sal]^-$). Using different ion pairs, the following AGB-ILs were investigated: *N,N,N*-triethyl(4-ethoxy-4-oxobutyl)-1-ammonium bromide, $[Et_3NC_4]Br$; *N,N,N*-tri(n-propyl)(4-ethoxy-4-oxobutyl)-1-ammonium bromide, $[Pr_3NC_4]Br$; *N,N,N*-tri(n-butyl)(4-ethoxy-4-oxobutyl)-1-ammonium bromide, $[Bu_3NC_4]Br$; 1-(4-ethoxy-4-oxobutyl)-1-methylpyrrolidin-1-ium bromide, $[MepyrNC_4]Br$; *N,N,N*-tri(*n*-propyl)(4-ethoxy-4-oxobutyl)-1-ammonium saccharinate, $[Pr_3NC_4][Sac]$; *N,N,N*-tri(*n*-propyl)(4-ethoxy-4-oxobutyl)-1-ammonium lactate, $[Pr_3NC_4][Lac]$; *N,N,N*-tri(*n*-propyl)(4-ethoxy-4-oxobutyl)-1-ammonium pyruvate, $[Pr_3NC_4][Pyr]$; *N,N,N*-tri(*n*-propyl)(4-ethoxy-4-oxobutyl)-1-ammonium dicyanamide, $[Pr_3NC_4][Dca]$; *N,N,N*-tri(*n*-propyl)(2-ethoxy-2-oxoethyl)-1-ammonium salicylate, $[Pr_3NC_2][Sal]$; and *N,N,N*-tri(*n*-propyl)(4-ethoxy-4-oxobutyl)-1-ammonium salicylate, $[Pr_3NC_4][Sal]$ (cf. Figure 1).

The synthesis, characterization and ecotoxicity of Br-based AGB-ILs have been previously reported, employing established methodologies such as ^1H and ^{13}C NMR,

elemental analysis, melting point determination, thermal decomposition analysis, and the Standard Microtox® liquid-phase bioassay [27]. In the present work, additional AGB-ILs incorporating alternative anions were synthesized and fully characterized to expand the structural spectrum of these compounds and to support a more comprehensive understanding of their physicochemical and toxicological profiles.

Structural confirmation and purity assessment of the newly reported AGB-ILs were performed using ^{1}H and ^{13}C NMR and elemental analysis, indicating >99 wt% purity and no detectable impurities. As for Br-based [27], the remaining AGB-ILs are liquid below 100 °C, with melting temperatures from 30.58 to 98.51 °C, and decomposition temperatures from 151.23 to 189.64 °C. All data confirming their chemical structure, purity, and thermal properties is provided in Table S2-S7 (Supplementary Material).

To evaluate the potential of AGB-ILs in greener sample preparation methods, with particular emphasis on compliance with principle 2 (*Use safer solvents and reagents*) [24], their ecotoxicity was evaluated toward *A. fischeri*. Full EC_{50} data after 5, 15, and 30 min are presented in Table S8 (Supplementary Material), confirming consistent toxicity trends across time points, with the 30-min values used for discussion to provide a conservative assessment. EC_{50} values ($mg.L^{-1}$) of the newly reported AGB-ILs decrease according to the following sequence, where a lower EC_{50} indicates higher toxicity: $[Pr_3NC_4][Lac]$ (1713.5) > $[Pr_3NC_4][Dca]$ (672.3) > $[Pr_3NC_4][Pyr]$ (646.5) > $[Pr_3NC_2][Sal]$ (304.7) > $[Pr_3NC_4][Sal]$ (137.5) > $[Pr_3NC_4][Sac]$ (38.6).

Despite sharing a common cationic backbone, AGB-ILs differ in carbon chain length and anion structure, allowing a dissection of their individual roles in toxicity. Longer carbon chains ($[Pr_3NC_2][Sal]$ vs. $[Pr_3NC_4][Sal]$) are responsible for an increased capacity to perturb or even disrupt cell membranes due to their enhanced hydrophobicity, resulting in a reduction of *A. fischeri* bioluminescence, in line with the well-established "side chain effect" [41]. Considering AGB-ILs with a common cation ($[Pr_3NC_4]^+$) but different anions, the substitution of an hydroxyl by a carbonyl group ($[Lac]^-$ vs. $[Pyr]^-$) and the incorporation of aromatic rings ($[Lac]^-$ vs. $[Sal]^-$ and $[Sac]^-$) enhance the toxicity of these compounds, consistent with some literature findings [41,42]. $[Dca]^-$, featuring a linear structure with –CN groups, exhibits lower toxicity compared to aromatic anions. In comparison, bromide, a simple halide anion, is the least toxic anion, with a reported EC_{50} value of 2018.7 $mg.L^{-1}$ for $[Pr_3NC_4]Br$ [27].

Apart from $[Pr_3NC_4][Sac]$, AGB-ILs were found to be non-toxic to *A. fischeri*, as indicated by their EC_{50} values at 30 min meeting the European Legislation criteria (EC_{50} > 100 $mg \cdot L^{-1}$) [43]. Compared to commercially available ILs, such as 1-butyl-3-methylimidazolium bromide (735.9 $mg.L^{-1}$ [44]), tetrabutylammonium bromide (128.6 $mg.L^{-1}$ [28]) and tetrabutylphosphonium bromide (172.8 $mg.L^{-1}$ [44]), AGB-ILs can be structurally tailored to display toxicity levels that are either comparable to or even lower than these reference compounds. These results showcase AGB-ILs as acceptable tools for depletion methods.

Aiming to establish mixture compositions for liquid-liquid extraction systems to be further applied in depletion studies, the ternary phase diagrams of ABS comprising AGB-ILs and citrate buffer were determined at 25 °C and atmospheric pressure. Figure 3 depicts the binodal curves for AGB-ILs + $K_3C_6H_5O_7/C_6H_8O_7$ + water systems at 25 °C and pH≈7. Related information, including ternary phase diagrams compositions (in weight fraction), Merchuk equation regression parameters and TL data is provided in Table S9-S12 (Supplementary Material). Data on Br-based AGB-ILs are reported elsewhere [27].

In all AGB-IL-based ABS, the biphasic zone lies above the solubility curve, whereas the monophasic region is below. A larger biphasic area indicates a greater ability to undergo liquid-liquid demixing, i.e., the AGB-IL is more readily salted-out by citrate salt. Figure 3A shows the effect of the cation alkyl chain length by comparing $[Pr_3NC_2][Sal]$ and $[Pr_3NC_4][Sal]$ systems. Consistent with general rules for IL-based ABS formation and previous observations with Br-based AGB-ILs [27], the longer-chain (i.e., $[Pr_3NC_4][Sal]$) is more prone to phase separation due its higher hydrophobicity, facilitating salting-out. In turn, Figure 3B shows the impact of the anion nature on ABS formation, which can be ranked as follows: $[Pr_3NC_4][Pyr]$ < $[Pr_3NC_4][Lac]$ < $[Pr_3NC_4]Br$ < $[Pr_3NC_4][Sal]$ ≈ $[Pr_3NC_4][Sac]$ < $[Pr_3NC_4][Dca]$. Aromatic ($[Sal]^-$ and $[Sac]^-$) and cyano-based anions ($[Dca]^-$) enhance ABS formation, whereas anions derived from monocarboxylic acids ($[Lac]^-$ and $[Pyr]^-$) limit liquid-liquid demixing.

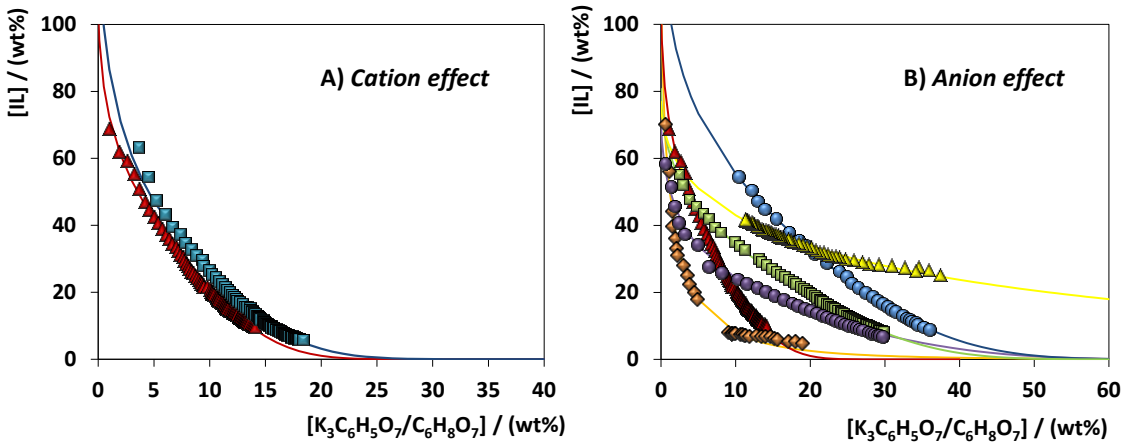

Figure 3. Binodal curves for ABS formed by AGB-IL + $K_3C_6H_5O_7/C_6H_8O_7$ + H_2O at 25 °C and pH 7: (A) $[Pr_3NC_2][Sal]$ (blue squares); $[Pr_3NC_4][Sal]$ (red triangles); (B) $[Pr_3NC_4][Pyr]$ (yellow triangles); $[Pr_3NC_4][Lac]$ (blue circles); $[Pr_3NC_4]Br$ (green squares) [27]; $[Pr_3NC_4][Sal]$ (red triangles); $[Pr_3NC_4]][Sac]$ (purple circles); $[Pr_3NC_4][Dca]$ (orange diamonds).

To further assess phase separation efficiency, TLLs were determined for all studied AGB-IL-based ABS at a fixed mixture composition (30/30 wt% AGB-IL/salt, highlighted in Table S12, Supplementary Material). Longer TLLs indicate a larger compositional difference between the AGB-IL-rich and salt-rich phases, generally correlating with enhanced phase separation. Within the cation series, the TLL increases in the order $[Pr_3NC_4][Lac]$ (77.73) < $[Pr_3NC_4][Pyr]$ (85.89) < $[Pr_3NC_4]Br$ (87.96) < $[Pr_3NC_4][Sal]$ (91.79) < $[Pr_3NC_4][Sac]$ (91.92) < $[Pr_3NC_4][Dca]$ (92.51), whereas, for a fixed anion, $[Pr_3NC_2][Sal]$ (88.92) exhibits a shorter TLL than $[Pr_3NC_4][Sal]$ (91.92). These results are consistent with the hydrophobic character of the AGB-ILs, as ILs with lower water affinity require less citrate salt to form ABS, yielding longer TLLs and more efficient phase separation.

Overall, combined analyses of structural and physicochemical characterization, favorable ecotoxicity and phase behavior indicate that more hydrophobic AGB-ILs efficiently form ABS, providing potential routes for protein removal and guiding the design of subsequent depletion workflows.

3.2. Depletion of high-abundance serum proteins using AGB-IL-based ABS

After appraising mixture compositions required to create AGB-IL-based ABS, their ability as serum protein depletion strategies was investigated. The depletion

efficiencies of HSA and IgG in all AGB-IL-based ABS were evaluated using a common mixture composition within the biphasic region. The composition consisted of 30 wt% of AGB-IL, 60 wt% of citrate buffer solution ($K_3C_6H_5O_7/C_6H_8O_7$ at 50 wt% in water, pH 7) and 10 wt% of human serum directly added to the system. To balance efficient protein precipitation with reduced sample and chemical usage, as advocated by principle 5 of Green Sample Preparation (*Minimize sample, chemical and material amounts*), a 2 g ABS mass comprising 10 wt% serum was employed [24].

In all systems, the top phase is AGB-IL-rich, whereas most of the salt prevails in the bottom phase. HSA and IgG were not detected in either aqueous phase, at least in concentrations above the LOD of SE-HPLC-UV, which corresponds to quantitative depletion as defined in the Materials and Methods. High-abundance serum proteins, once depleted, constitute most of the solid interphase. The results obtained are summarized in Table S13 (Supplementary Material).

All AGB-IL-based ABS achieved efficient depletion of high-abundance serum proteins in a single step. This is consistent with their rational design based on enhanced hydrophobicity combined with water miscibility, which is a key requirement for ABS formation. The intrinsic hydrophobic character may drive HSA and IgG precipitation at the interphase, promoting protein-protein interactions and aggregation under low-water conditions, as previously observed in other ABS [21]. Although the quantitative precipitation of HSA and IgG may result from denaturation or changes in their structural state, this phenomenon does not impact the downstream detection of biomarkers.

It should be further noticed that all systems were investigated at a fixed biphasic composition and present well-defined AGB-IL-rich and salt-rich phases. However, $[Pr_3NC_4][Sac]$ and $[Pr_3NC_4][Dca]$ deviate from this behavior, leading to the formation of a large solid interphase, with a jellified AGB-IL-rich phase. This jellification is dependent on the AGB-IL chemical structure under the studied conditions. The $[Pr_3NC_4][Sac]$ and $[Pr_3NC_4][Dca]$ are among the most hydrophobic AGB-ILs studied, as reflected by both their ability to form ABS (Figure 3) and the relatively long TLLs achieved (Table S12, Supplementary Material). The water content in the AGB-IL-rich phase of these systems at the studied compositions is relatively low (<20 wt%), which may account for the observed jellification of this phase. Consequently, such systems are technically unsuitable for bioanalytical applications.

The depletion efficiencies achieved with AGB-IL-based ABS surpass those reported for most commercial depletion columns and kits, including those based on dye-affinity, protein ligands and/or immunoaffinity, as well as chemical precipitation and other types of ABS (e.g., polymeric, micellar and commercial IL-based systems), as summarized in Table 1. Dye-ligand affinity and protein ligand affinity columns are considered the gold standard for the depletion of HSA and IgG, respectively [45,46]; yet, the development of hybrid technologies is required if depletion of other high-abundance proteins is needed [9]. Most commercial kits can simultaneously deplete various proteins using distinct types of affinity resins and columns. However, these are limited by: (i) multiple and lengthy equilibration, adsorption and/or desorption tasks (40 min - >2 hours); (ii) overpriced protein- and immunoaffinity-ligands; (iii) low sample loading capacities (10-50 µL); and (iv) low yields [47]. By using ILs inspired by naturally occurring compounds and a biodegradable salt, AGB-IL-based ABS could overcome these issues providing an efficient depletion of both HSA and IgG using 0.1 g of serum per g of system in a fast workflow.

Due to its technological simplicity, chemical precipitation of high-abundance proteins is widely employed either alone or in combination with immunoaffinity methods [48]; yet, co-precipitation events, low yields, resolubilization, and lengthy protocols are recurrent [9]. AGB-IL-based ABS allow higher depletion efficiencies in a single step while replacing volatile organic solvents or their mixtures (e.g., methanol, acetone, chloroform, acetonitrile) with water, a biodegradable organic salt, and non-toxic ILs [48].

As compared with commonly used ABS, namely those based on polyethylene glycol and dextran or surfactants, the incorporation of AGB-ILs leads to the simultaneous depletion of HSA and IgG to a much higher extent [11,19]. Compared to commercially available ILs belonging to imidazolium, tetraalkylammonium and phosphonium families, AGB-ILs demonstrate a more satisfactory balance between performance and toxicity. Among the reference ILs, only tetrabutylphosphonium bromide exhibits comparable protein depletion capacity, but with higher toxicity limits [21]. Tetrabutylammonium bromide is not only more toxic than most AGB-ILs but also less efficient in protein depletion [21]. Furthermore, 1-butyl-3-methylimidazolium bromide, one of the most

widely studied commercial ILs, fails to deplete serum proteins via interfacial precipitation due to its higher hydrophilic character [21].

Table 1. Critical assessment of common methods for protein depletion from human serum.

Depletion technique	**Trade name**	**Description**	**Proteins depleted**	**Sample loading**	**Processing time**	**Detection method compatibility**	**Depletion efficiency**	**Manufacturer/Reference**
Dye-ligand affinity	HiTrap™ Blue column	Affi-gel blue column where cibacron blue is linked to Sepharose	HSA	50-200 mL	Not specified	Electrophoresis and ion exchange chromatography	98 % (HSA)	GE Healthcare Life Sciences/[45]
Protein ligand affinity	HiTrap™ Protein G column	Protein G Sepharose	Igs	≈2 mL	Not specified	Not specified	100 % (Igs)	GE Healthcare Life Sciences/[46]
Immunoaffinity	Pierce™ Top 2 Abundant Protein Depletion Spin Columns	Anti-HSA and anti-IgG antibodies immobilized onto spin columns	HSA, IgG	10 µL	≈40 min	1-D or 2-D gel electrophoresis and mass spectrometry	> 95 % (HSA); > 90 % (IgG)	Thermo Fisher Scientific/[47]
Immunoaffinity	Pierce™ Top 12 Abundant Protein	Highly specific antibodies immobilized onto spin columns	HSA, IgG + 10 high-abundance	10 µL	≈60 min	1-D or 2-D gel electrophoresis and mass	> 95 % (all proteins)	Thermo Fisher Scientific/[47]

	Depletion Spin Columns		proteins			spectrometry		
Immunoaffinity	Albumin and IgG Depletion SpinTrap™	Mixture of anti-HSA high performance sepharose and Protein G Sepharose	HSA, IgG	25 µL	Not specified	1-D or 2-D gel electrophoresis and mass spectrometry	> 95 % (HSA); > 90 % (IgG)	GE Healthcare/[47]
Immunoaffinity	Proteo Prep® Immunoaffinity Albumin & IgG Depletion Kit	Columns consisting of a mixture of two beaded mediums containing recombinantly expressed, small single-chain antibody ligands	HSA, IgG	25-50 µL	Not specified	Two-dimensional electrophoresis or liquid chromatography	> 95 % (HSA); 85 % (IgG)	Sigma-Aldrich/[47]
Dye- and protein-ligand affinity	Pierce™ Albumin/IgG Removal Kit	Cibacron Blue Dye and Protein A agarose affinity resin	HSA, IgG	10 µL	≈40 min	Western blotting, 2D electrophoresis or 2D-LC mass spectrometry	≈100 % (HSA); ≈100 % (IgG)	Thermo Fisher Scientific/[47]
Combinatorial library of hexape	ProteoMiner protein enrich	Bead features a different hexapeptide ligand with	High-abundance	40 µL	>2 hours	Mass spectrometry	Nearly all proteins	Bio-Rad/[47]

ptides-ligand affinity	ment kit	affinity for specific proteins	prot eins					
Chemical Precipitation	Not applicable	Organic solvents or their mixtures	Serum proteins (not specified)	100 µL.(300-900 µL of organic solvent)$^{-1}$	Not specified	Mass spectrometry	< 90 % (based on 10 % of HSA that did not precipitate)	Not applicable/[48]
Micellar ABS	Not applicable	Triton X-114 + SDS	HSA	0.1 mL.(10mL of ABS)$^{-1}$	15 min	SDS-PAGE	95 % (HSA)	Not applicable/[11]
Polymeric ABS	Not applicable	Polyethylene glycol + dextran	Total Proteins	1 mg.(500 µg of ABS)$^{-1}$	15 min	PCR	77.5 % (based on total proteins)	Not applicable/[19]
Commercial IL-based ABS	Not applicable	Imidazolium-based, tetraalkylammonium-based and tetrabutylphosphonium-based ILs + K_2HPO_4/KH_2PO_4 (pH = 7)	HSA; IgG	0.1 g.(g of ABS)$^{-1}$	20 min	SE-HPLC-UV	0 – 99 % (HSA); 0 – 100 % (IgG)	Not applicable/[21]
AGB-IL-based ABS	Not applicable	AGB-IL + $K_3C_6H_5O_7$/$C_6H_8O_7$ (pH = 7)	HSA; IgG	0.1 g.(g of ABS)$^{-1}$	20 min	SE-HPLC-UV; SDS-PAGE	Quantitative depletion	Not applicable/ This work

3.3. ABS-mediated detection of target protein biomarkers

As discussed above, AGB-IL-based ABS exhibited high performance in depleting HSA and IgG from human serum, outperforming both conventional approaches and other ABS formulations tested. This, in turn, improved the detectability of target proteins in serum by SE-HPLC-UV, as shown in Figure 4.

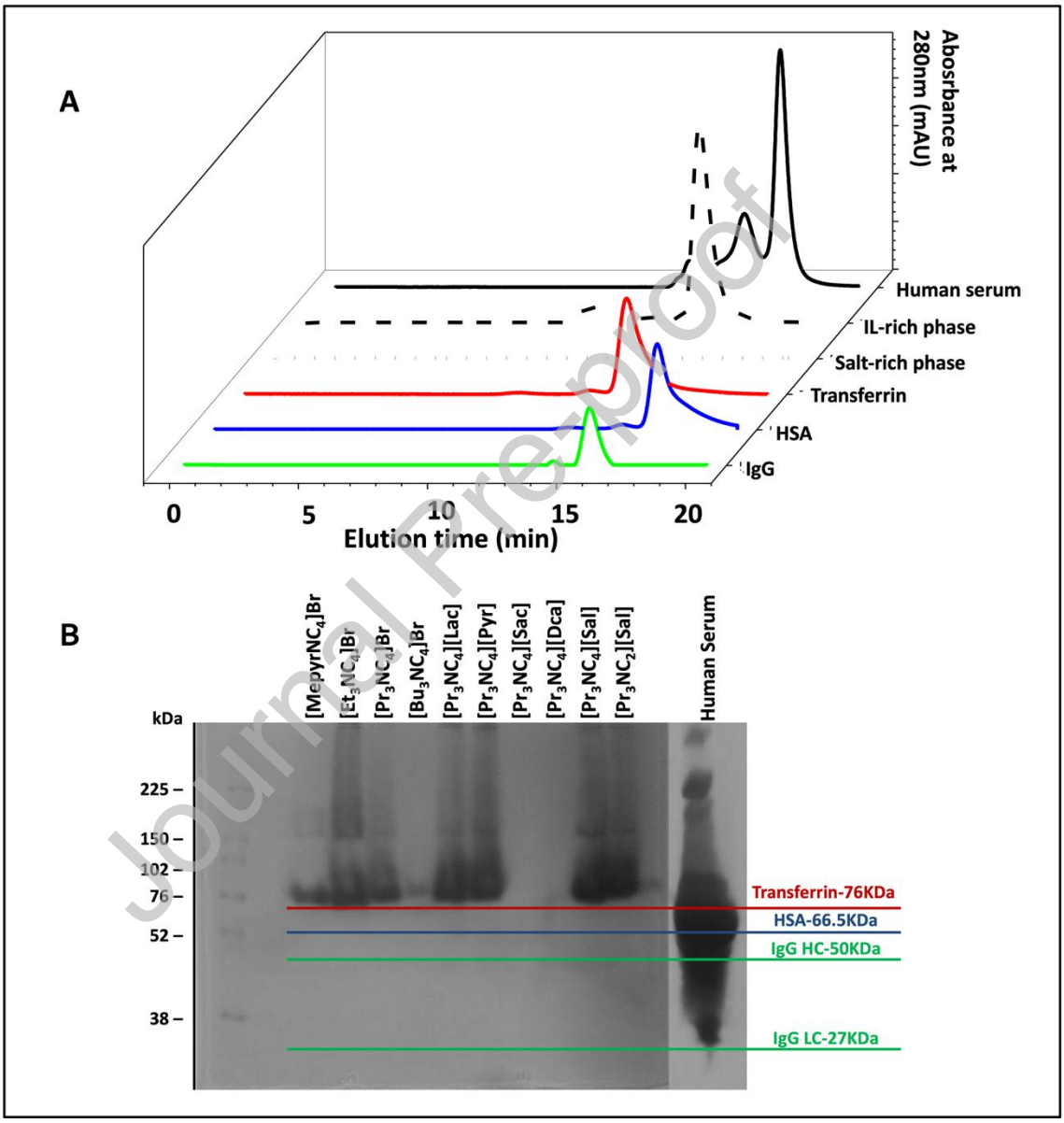

Figure 4. Characterization of serum protein depletion performance with AGB-IL-based ABS: (A) Representative SE-HPLC-UV chromatograms for human serum in PBS [1:10 (v/v)], ABS phases of the system composed of 30 wt% of $[Bu_3NC_4]Br$ + 60 wt% of citrate buffer ($K_3C_6H_5O_7/C_6H_8O_7$ at 50 wt%, pH 7) + 10 wt% of human serum, transferrin

standard solution (1 g·L^{-1}), HSA standard solution (1 g·L^{-1}) and IgG standard solution (0.5 g·L^{-1}); (B) SDS-PAGE of proteins on the AGB-IL-rich phase of ABS.

Although SE-HPLC-UV may not detect trace residual HSA and IgG in the AGB-IL-rich phase, the observed quantitative depletion eliminates interference from these high-abundance serum proteins. This allowed a new peak, not visible without the sample pretreatment, to be detected, enabling the subsequent detection of target proteins present at lower concentrations (cf. Figure 4A). To validate this assumption, the AGB-IL-rich phase was analyzed by SDS-PAGE to identify the protein newly unmasked following the depletion step. According to the molecular weight and serum proteomic profile, the SDS-PAGE results depicted in Figure 4B allow identifying the unknown protein as transferrin, which is also a promising biomarker. Besides, while the detected concentration of transferrin in the AGB-IL-rich phase was below the estimated LOQ, a recovery yield of 78% from serum was achieved using the [Bu_3NC_4]Br-based ABS, corresponding to 1.42 g·L^{-1} compared to 1.8 g·L^{-1} in the original sample. This reduction of matrix effects supports SE-HPLC-UV compatibility, with the AGB-IL-rich phase remaining suitable for analysis upon dilution. In general, compatibility with downstream analytical techniques should be considered, as IL-rich phases may require dilution or additional clean-up steps to ensure optimal analytical performance, depending on the selected platform.

Transferrin was further quantified with a relative error of 22% compared to ELISA measurements of the original serum (see Table S14, Supplementary Material). While this error exceeds the ±15% acceptance criteria for bioanalytical method validation [49], it demonstrates a promising starting point for further optimization.

Transferrin is an iron-binding glycoprotein of clinical relevance in anemia and alcoholism evaluation, also holding promise in cancer early diagnosis [50]. Even though it is not a low-abundance protein, and biomarkers at the typical ng·L^{-1} to pg·L^{-1} range remain below the LODs of SE-HPLC-UV without pre-concentration, the method can still serve as an efficient sample clean-up step. This results in the selective analysis of target proteins that would otherwise remain undetectable, highlighting the practical utility of SE-HPLC-UV in the analysis complex biological samples.

Reports on the detection of serum transferrin by mass spectrometry resorted to commercial depletion kits (e.g., ProteoPrep®) [51], while ELISA-based quantification has also been widely used [52]. In this context, AGB-IL-based ABS provide efficient depletion while streamlining serum pretreatment strategies. Their ability to unmask human transferrin allows its subsequent detection by SE-HPLC-UV, reducing reliance on mass spectrometry or immunoassays. SE-HPLC-UV provides a simpler and more cost-effective analytical platform, which is highly advantageous for clinical applications requiring rapid and accessible protein quantification.

3.4. Green assessment of AGB-IL-based ABS for unmasking target proteins in SE-HPLC-UV

Alongside the analytical performance, outcomes relative to reported workflows, and the low toxicity of AGB-ILs, a comprehensive green assessment is warranted to validate the method's sustainability claims. To this aim, three complementary metrics were adopted to quantitatively examine aspects such as sample throughput, reagent minimization, energy consumption, and waste generation: the AGREE metric (Analytical GREEnness), providing an overall evaluation of compliance with Green Analytical Chemistry principles [31]; the AGREEprep metric, derived from AGREE and specifically focused on the sample preparation stage [32]; and the Blue Applicability Grade Index (BAGI), a complementary tool focused on the practical, application-driven dimensions of White Analytical Chemistry [33]. Figure 5 summarizes the scores of these evaluations.

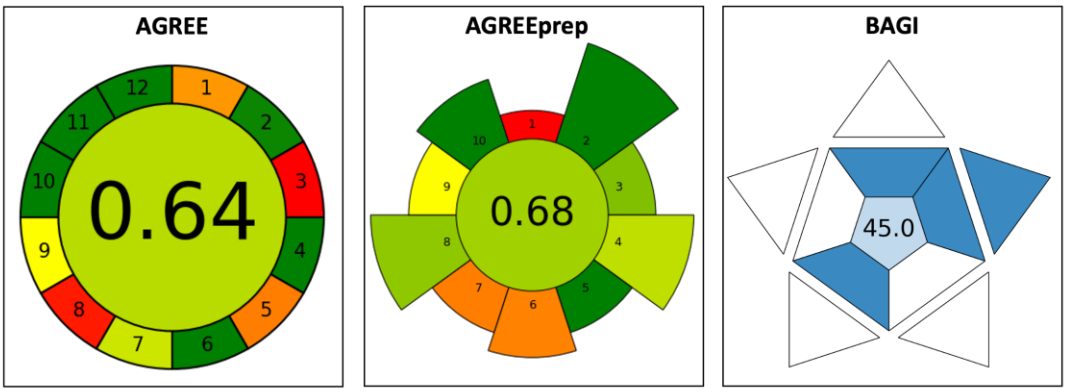

Figure 5. Green assessment of AGB-IL-based ABS applied to target protein unmasking in SE-HPLC-UV using AGREE [31], AGREEprep [32], and BAGI [33] metric tools. Circular diagrams represent the AGREE and AGREEprep scores, where the green-shaded area indicates compliance with Green Analytical Chemistry [31] or Green Sample Preparation [24] principles, ranging from 0 (poor alignment) to 1 (full compliance). For BAGI, an asteroid pictogram is presented, with shades of blue representing the score intensity (darker blue = higher applicability), together with the respective numerical score, reflecting alignment with White Analytical Chemistry principles [33].

Based on AGREE (score 0.64), AGREEprep (score 0.68), and BAGI (score 45) evaluations, the proposed AGB-IL-based ABS workflow shows a reasonable balance of green and operational considerations for target protein analysis in serum. According to AGREE [31], high scores are expected for sample amount reduction (criterion 2), minimization of reagents and processing steps (criterion 4), avoidance of derivatization (criterion 6), limitation of waste generation (criterion 7), and operator safety (criteria 10-12). Moderate scores arise from sample pretreatment and batch operation (criterion 1) and limited automation and miniaturization (criterion 5). Lower scores are associated with energy consumption from centrifugation, mixing, and HPLC analysis (criterion 9). They also indicate off-line analysis with limited throughput, arising from the single-analyte workflow and 40 min SE-HPLC-UV runs (criteria 3 and 8).

A more detailed evaluation of the sample preparation step using AGREEprep highlights the environmental performance of AGB-IL-based ABS, with strong scores for reagent choice (criteria 2 and 3), low waste (criterion 4), small sample size (criterion 5), energy efficiency (criterion 8), and operator safety (criterion 10) [32]. Moderate scores reflect limited throughput (criterion 6), manual operation (criterion 7), and post-pretreatment HPLC analysis (criterion 9), with the main penalty from criterion 1 due to ex situ sample preparation. Complementing these assessments, the BAGI score suggests analytical accessibility and biological relevance, enabling single-analyte quantification of transferrin with readily available instrumentation [33]. Limitations mirror those identified by AGREE and AGREEprep (low throughput and partial automation), resulting in a moderate overall applicability.

Overall, the low toxicity observed for the AGB-ILs (Section 3.1) supports principle 2 of Green Sample Preparation (*Use safer solvents and reagents*) [24] and aligns with the objectives of Green Analytical Chemistry [31], reinforcing operator safety and the use of environmentally benign reagents. This is also shown in the BAGI evaluation, where reagent safety and environmental impact contribute to the assessment of the method's bioanalytical sustainability. Opportunities for improvement include automation, workflow integration, and reagent/material reuse, which could further enhance operational efficiency and analytical applicability.

4. Conclusions

This work demonstrates that AGB-IL-based ABS can be successfully applied as efficient serum protein depletion strategies through the selective removal of high-abundance species. This process creates the analytical conditions required for biomarker detection using expedited analytical techniques. AGB-ILs were synthesized, characterized, and combined with a citrate buffer to form ABS in accordance with Green Sample Preparation principles.

The low water affinity of AGB-ILs was translated into highly efficient depletion of HSA and IgG from human serum, resulting in the detection of target proteins that would otherwise remain masked. Direct analysis of transferrin in untreated serum by SE-HPLC-UV was not feasible due to the high abundance of HSA and IgG, which dominate the chromatographic signal and mask its peak. By extracting target proteins into the AGB-IL-rich phase, SE-HPLC-UV detection was achieved in an expedited manner. These results show that appropriate sample pretreatment enables serum protein detection using simpler analytical techniques, offering a complementary strategy to established methods such as immunoassays or mass spectrometry.

Combined AGREE, AGREEprep, and BAGI assessments further suggest that the ABS-mediated sample pretreatment aligns with green and safe practices, while indicating moderate practical applicability and highlighting opportunities for improvement through automation, workflow integration, and material reuse.

Overall, the findings highlight the potential of AGB-IL-based ABS as sustainable tools for bioanalytical workflows, combining Green and White Analytical Chemistry principles with improved sample pretreatment and biomarker detection.

Credit authorship contribution statement

M.M.P.: Methodology, Validation, Formal analysis, Investigation, Data Curation, Visualization, Writing-original draft; S.N.P.: Formal analysis, Investigation, Data Curation; F.A.eS.: Methodology, Visualization, Writing – review & editing, Funding Acquisition; A.M.: Methodology, Resources, Supervision; J.A.P.C.: Conceptualization, Writing – review & editing, Supervision; M.G.F.: Conceptualization, Writing – review & editing, Supervision, Funding Acquisition, Project Administration.

Acknowledgements

This work was developed within the scope of the project CICECO – Aveiro Institute of Materials, UID/50011/2025 (DOI 10.54499/UID/50011/2025) & LA/P/0006/2020 (DOI 10.54499/LA/P/0006/2020), financed by national funds through the FCT/MCTES (PIDDAC). This work was funded by national funds (OE) through FCT/MCTES from the project ILSurvive, PTDC/EMD-TLM/3253/2020 (DOI 10.54499/PTDC/EMD-TLM/3253/2020) and by FEDER through the COMPETE 2020 Programme and National Funds through FCT – Portuguese Foundation for Science and Technology under the project NANOBIOSENSE, POCI-01-0145-FEDER-028755. The NMR spectrometers are part of the National NMR Network (PTNMR) and are partially supported by Infrastructure Project Nº 022161 (co-financed by FEDER through COMPETE 2020, POCI and PORL and FCT through PIDDAC). Francisca A. e Silva acknowledges FCT for the researcher contract CEECIND/03076/2018/CP1559/CT0024 (DOI 10.54499/CEECIND/03076/2018/CP1559/CT0024) under the Scientific Employment Stimulus – Individual Call 2018.

Declaration of competing interest

The authors declare that they have no known competing financial interests or personal relationships that could have appeared to influence the work reported in this paper.

Data availability

Data will be made available on request.

References

[1] N.G. Frangogiannis, Biomarkers: Hopes and challenges in the path from discovery to clinical practice, Transl. Res. 159 (2012) 197–204. https://doi.org/10.1016/j.trsl.2012.01.023.

[2] K. Chandramouli, P.-Y. Qian, Proteomics: Challenges, Techniques and Possibilities to Overcome Biological Sample Complexity, Hum. Genomics Proteomics. 1 (2009) 239204.

[3] Y. Jmeian, Z. El Rassi, Liquid-phase-based separation systems for depletion, prefractionation and enrichment of proteins in biological fluids for in-depth proteomics analysis, Electrophoresis. 30 (2009) 249–261. https://doi.org/10.1002/elps.200800639.

[4] R. Mayeux, Biomarkers: Potential Uses and Limitations, NeuroRx. 1 (2004) 182–188. https://doi.org/10.1602/neurorx.1.2.182.

[5] N.L. Anderson, N.G. Anderson, The human plasma proteome: history, character, and diagnostic prospects., Mol. Cell. Proteomics. 1 (2002) 845–867. https://doi.org/10.1074/mcp.R200007-MCP200.

[6] K. Mariño, R. Saldova, B. Adamczyk, P.M. Rudd, Changes in serum N-glycosylation profiles: Functional significance and potential for diagnostics, Carbohydr. Chem. 37 (2011) 57–93. https://doi.org/10.1039/9781849732765-00057.

[7] L. Wu, X. Qu, Cancer biomarker detection: Recent achievements and challenges, Chem. Soc. Rev. 44 (2015) 2963–2997. https://doi.org/10.1039/c4cs00370e.

[8] S.B. Nimse, M.D. Sonawane, K.S. Song, T. Kim, Biomarker detection technologies and future directions, Analyst. 141 (2016) 740–755. https://doi.org/10.1039/c5an01790d.

[9] P.Y. Lee, J. Osman, T.Y. Low, R. Jamal, Plasma/serum proteomics: Depletion strategies for reducing high-abundance proteins for biomarker discovery, Bioanalysis. 11 (2019) 1799–1812. https://doi.org/10.4155/bio-2019-0145.

[10] A. Tomascova, J. Lehotsky, D. Kalenska, E. Baranovicova, P. Kaplan, Z. Tatarkova, A comparison of albumin removal procedures for proteomic analysis of blood plasma, Gen. Physiol. Biophys. 38 (2019) 305–314. https://doi.org/10.4149/gpb_2019009.

[11] M.A.O. da Silva, M.A.Z. Arruda, An aqueous two-phase system as a strategy for serum albumin depletion, Talanta. 77 (2009) 985–990. https://doi.org/10.1016/j.talanta.2008.07.055.

[12] A.M.S. Jorge, J.F.B. Pereira, Aqueous two-phase systems – versatile and advanced (bio)process engineering tools, Chem. Commun. (2024). https://doi.org/10.1039/D4CC02663B.

[13] F.D. Raymond, D.W. Moss, D. Fisher, Separation of alkaline phosphatase isoforms with and without intact glycan-phosphatidylinositol anchors in aqueous polymer phase systems, Clin. Chim. Acta. 227 (1994) 111–120. https://doi.org/10.1016/0009-8981(94)90140-6.

[14] R.Y.T. Chiu, A. V. Thach, C.M. Wu, B.M. Wu, D.T. Kamei, An aqueous two-phase system for the concentration and extraction of proteins from the interface for detection using the lateral-flow immunoassay, PLoS One. 10 (2015) e0142654. https://doi.org/10.1371/journal.pone.0142654.

[15] A.B. Simon, J.P. Frampton, N.-T. Huang, K. Kurabayashi, S. Paczesny, S. Takayama, Aqueous two-phase systems enable multiplexing of homogeneous immunoassays, Technology. 2 (2014) 176–184. https://doi.org/10.1142/s2339547814500150.

[16] J.P. Frampton, J.B. White, A.B. Simon, M. Tsuei, S. Paczesny, S. Takayama, Aqueous two-phase system patterning of detection antibody solutions for cross-reaction-free multiplex ELISA, Sci. Rep. 4 (2014) 4878. https://doi.org/10.1038/srep04878.

[17] J. Kim, H. Shin, J. Kim, J. Kim, J. Park, Isolation of high-purity extracellular vesicles by extracting proteins using aqueous two-phase system, PLoS One. 10 (2015) e0129760. https://doi.org/10.1371/journal.pone.0129760.

[18] H. Shin, Y.H. Park, Y.G. Kim, J.Y. Lee, J. Park, Aqueous two-phase system to isolate extracellular vesicles from urine for prostate cancer diagnosis, PLoS One. 13 (2018) e0194818. https://doi.org/10.1371/journal.pone.0194818.

[19] H. Shin, C. Han, J.M. Labuz, J. Kim, J. Kim, S. Cho, Y.S. Gho, S. Takayama, J. Park, High-yield isolation of extracellular vesicles using aqueous two-phase system, Sci. Rep. 5 (2015) 13103. https://doi.org/10.1038/srep13103.

[20] S.Y. Lee, I. Khoiroh, C.W. Ooi, T.C. Ling, P.L. Show, Recent Advances in Protein Extraction Using Ionic Liquid-based Aqueous Two-phase Systems, Sep. Purif. Rev. 46 (2017) 291–304. https://doi.org/10.1080/15422119.2017.1279628.

[21] M.E. Rosa, M.S.M. Mendes, E. Carmo, J.P. Conde, J.A.P. Coutinho, M.G. Freire, F.A. e Silva, Tailored pretreatment of serum samples and biomarker extraction afforded by ionic liquids as constituents of aqueous biphasic systems, Sep. Purif. Technol. 322 (2023) 124248. https://doi.org/10.1016/j.seppur.2023.124248.

[22] Z. Li, X. Liu, Y. Pei, J. Wang, M. He, Design of environmentally friendly ionic liquid aqueous two-phase systems for the efficient and high activity extraction of proteins, Green Chem. 14 (2012) 2941. https://doi.org/10.1039/c2gc35890e.

[23] A. Basaiahgari, V.P. Priyanka, S.P. Ijardar, R.L. Gardas, Aqueous biphasic systems of amino acid-based ionic liquids: Evaluation of phase behavior and extraction capability for caffeine, Fluid Phase Equilib. 506 (2020) 112373. https://doi.org/10.1016/j.fluid.2019.112373.

[24] Á.I. López-Lorente, F. Pena-Pereira, S. Pedersen-Bjergaard, V.G. Zuin, S.A. Ozkan, E. Psillakis, The ten principles of green sample preparation, TrAC Trends Anal. Chem. 148 (2022) 116530. https://doi.org/10.1016/j.trac.2022.116530.

[25] M. Espino, M. de los Ángeles Fernández, F.J.V. Gomez, M.F. Silva, Natural designer solvents for greening analytical chemistry, TrAC Trends Anal. Chem. 76 (2016) 126–136. https://doi.org/10.1016/j.trac.2015.11.006.

[26] A. Le Donne, E. Bodo, Cholinium amino acid-based ionic liquids, Biophys. Rev. 13 (2021) 147–160. https://doi.org/10.1007/s12551-021-00782-0.

[27] M.M. Pereira, S.N. Pedro, J. Gomes, T.E. Sintra, S.P.M. Ventura, J.A.P. Coutinho,

M.G. Freire, A. Mohamadou, Synthesis and characterization of analogues of glycine-betaine ionic liquids and their use in the formation of aqueous biphasic systems, Fluid Phase Equilib. 494 (2019) 239–245. https://doi.org/10.1016/j.fluid.2019.05.001.

[28] M.M. Pereira, M.R. Almeida, J. Gomes, A.F.C.S. Rufino, M.E. Rosa, J.A.P. Coutinho, A. Mohamadou, M.G. Freire, Glycine-betaine ionic liquid analogues as novel phase-forming components of aqueous biphasic systems, Biotechnol. Prog. 34 (2018) 1205–1212. https://doi.org/10.1002/btpr.2685.

[29] Y. Chen, T. Mu, Revisiting greenness of ionic liquids and deep eutectic solvents, Green Chem. Eng. 2 (2021) 174–186. https://doi.org/10.1016/j.gce.2021.01.004.

[30] S. Zhang, H. He, Q. Zhou, X. Zhang, X. Lu, Y. Tian, Principles and strategies for green process engineering, Green Chem. Eng. 3 (2022) 1–4. https://doi.org/10.1016/j.gce.2021.11.008.

[31] F. Pena-Pereira, W. Wojnowski, M. Tobiszewski, AGREE—Analytical GREEnness Metric Approach and Software, Anal. Chem. 92 (2020) 10076–10082. https://doi.org/10.1021/acs.analchem.0c01887.

[32] W. Wojnowski, M. Tobiszewski, F. Pena-Pereira, E. Psillakis, AGREEprep – Analytical greenness metric for sample preparation, TrAC Trends Anal. Chem. 149 (2022) 116553. https://doi.org/10.1016/j.trac.2022.116553.

[33] N. Manousi, W. Wojnowski, J. Płotka-Wasylka, V. Samanidou, Blue applicability grade index (BAGI) and software: a new tool for the evaluation of method practicality, Green Chem. 25 (2023) 7598–7604. https://doi.org/10.1039/D3GC02347H.

[34] A. Gałuszka, Z. Migaszewski, J. Namieśnik, The 12 principles of green analytical chemistry and the SIGNIFICANCE mnemonic of green analytical practices, TrAC Trends Anal. Chem. 50 (2013) 78–84. https://doi.org/10.1016/j.trac.2013.04.010.

[35] P.M. Nowak, R. Wietecha-Posłuszny, J. Pawliszyn, White Analytical Chemistry: An approach to reconcile the principles of Green Analytical Chemistry and functionality, TrAC Trends Anal. Chem. 138 (2021) 116223. https://doi.org/10.1016/j.trac.2021.116223.

[36] A. Messadi, A. Mohamadou, S. Boudesocque, L. Dupont, P. Fricoteaux, A. Nguyen-Van-Nhien, M. Courty, Syntheses and characterisation of hydrophobic ionic

liquids containing trialkyl(2-ethoxy-2-oxoethyl)ammonium or N-(1-methylpyrrolidyl-2-ethoxy-2- oxoethyl)ammonium cations, J. Mol. Liq. 184 (2013) 68–72. https://doi.org/10.1016/j.molliq.2013.04.023.

[37] Microbics Corporation, Microtox® Manual. A Toxicity Testing Handbook., (1992).

[38] J.C. Merchuk, B.A. Andrews, J.A. Asenjo, Aqueous two-phase systems for protein separation Studies on phase inversion, J. Chromatogr. B Anal. Technol. Biomed. Life Sci. 711 (1998) 285–293. https://doi.org/10.1007/s10953-016-0547-x.

[39] E. Alvarez-Guerra, S.P.M. Ventura, M. Alvarez-Guerra, J.A.P. Coutinho, A. Irabien, Modeling of the binodal curve of ionic liquid/salt aqueous systems, Fluid Phase Equilib. 426 (2016) 10–16. https://doi.org/10.1016/j.fluid.2016.01.004.

[40] N.V. Bhagavan, C.-E. Ha, Metabolism of Iron and Heme, in: Essentials Med. Biochem., Elsevier, 2015: pp. 511–529. https://doi.org/10.1016/B978-0-12-416687-5.00027-0.

[41] S. Stolte, M. Matzke, J. Arning, A. Böschen, W.-R. Pitner, U. Welz-Biermann, B. Jastorff, J. Ranke, Effects of different head groups and functionalised side chains on the aquatic toxicity of ionic liquids, Green Chem. 9 (2007) 1170. https://doi.org/10.1039/b711119c.

[42] N. Ferlin, M. Courty, S. Gatard, M. Spulak, B. Quilty, I. Beadham, M. Ghavre, A. Haiß, K. Kümmerer, N. Gathergood, S. Bouquillon, Biomass derived ionic liquids: synthesis from natural organic acids, characterization, toxicity, biodegradation and use as solvents for catalytic hydrogenation processes, Tetrahedron. 69 (2013) 6150–6161. https://doi.org/10.1016/j.tet.2013.05.054.

[43] United Nations, Part 4 – Environmental Hazards, (2009). https://www.unece.org/fileadmin/DAM/trans/danger/publi/ghs/ghs_rev01/English/04e_part4.pdf (accessed April 2, 2020).

[44] S.P.M. Ventura, C.S. Marques, A.A. Rosatella, C.A.M. Afonso, F. Gonçalves, J.A.P. Coutinho, Toxicity assessment of various ionic liquid families towards Vibrio fischeri marine bacteria, Ecotoxicol. Environ. Saf. 76 (2012) 162–168. https://doi.org/10.1016/j.ecoenv.2011.10.006.

[45] J. Travis, J. Bowen, D. Tewksbury, D. Johnson, R. Pannell, Isolation of albumin from whole human plasma and fractionation of albumin depleted plasma, Biochem. J. 157 (1976) 301–306. https://doi.org/10.1042/bj1570301.

[46] E.S. Bergmann-Leitner, R.M. Mease, E.H. Duncan, F. Khan, J. Waitumbi, E. Angov, Evaluation of immunoglobulin purification methods and their impact on quality and yield of antigen-specific antibodies, Malar. J. 7 (2008) 129. https://doi.org/10.1186/1475-2875-7-129.

[47] S. Pisanu, G. Biosa, L. Carcangiu, S. Uzzau, D. Pagnozzi, A human proteomic dataset from untreated and depleted/enriched serum samples, Data Br. 19 (2018) 1765–1767. https://doi.org/10.1016/j.dib.2018.06.042.

[48] T.M. Alshammari, A.A. Al-Hassan, T.B. Hadda, M. Aljofan, Comparison of different serum sample extraction methods and their suitability for mass spectrometry analysis, Saudi Pharm. J. 23 (2015) 689–697. https://doi.org/10.1016/j.jsps.2015.01.023.

[49] FDA, Bioanalytical Method Validation, (2018). https://www.fda.gov/files/drugs/published/Bioanalytical-Method-Validation-Guidance-for-Industry.pdf (accessed October, 2025).

[50] M.E. Elsayed, M.U. Sharif, A.G. Stack, Transferrin Saturation: A Body Iron Biomarker, in: Adv. Clin. Chem., Academic Press Inc., 2016: pp. 71–97. https://doi.org/10.1016/bs.acc.2016.03.002.

[51] Y. Yu, J. Xu, Y. Liu, Y. Chen, Quantification of human serum transferrin using liquid chromatography-tandem mass spectrometry based targeted proteomics, J. Chromatogr. B Anal. Technol. Biomed. Life Sci. 902 (2012) 10–15. https://doi.org/10.1016/j.jchromb.2012.06.006.

[52] M.A. Fernandes, G. Hanck-Silva, F.G. Baveloni, J.A. Oshiro Junior, F.T. de Lima, J.O. Eloy, M. Chorilli, A Review of Properties, Delivery Systems and Analytical Methods for the Characterization of Monomeric Glycoprotein Transferrin, Crit. Rev. Anal. Chem. (2020) 1–12. https://doi.org/10.1080/10408347.2020.1743639.

Declaration of interests

☒ The authors declare that they have no known competing financial interests or personal relationships that could have appeared to influence the work reported in this paper.

☐ The authors declare the following financial interests/personal relationships which may be considered as potential competing interests: